

# Deep Reinforcement Learning with Modulated Hebbian plus Q Network Architecture

Pawel Ladosz<sup>1</sup>, Eseoghene Ben-Iwhiwhu<sup>1</sup>, Yang Hu<sup>2</sup>, Nicholas Ketz<sup>3</sup>, Soheil Kolouri<sup>3</sup>,  
Jeffrey L. Krichmar<sup>4</sup>, Praveen Pilly<sup>3</sup> and Andrea Soltoggio<sup>1</sup>

<sup>1</sup> Department of Computer Science, Loughborough University, Loughborough, UK  
p.ladosz2@lboro.ac.uk, E.Ben-Iwhiwhu@lboro.ac.uk, a.soltoggio@lboro.ac.uk

<sup>2</sup> WMG, University of Warwick, Coventry CV4 7AL, UK  
yang.hu.1@warwick.ac.uk

<sup>3</sup> HRL Laboratories, 3011 Malibu Canyon Rd, Malibu, CA 90265  
naketz@hrl.com, Skolouri@hrl.com, pkpilly@hrl.com

<sup>4</sup> Department of Cognitive Sciences, Department of Computer Science, University of California, Irvine,  
Irvine, CA, 92697, USA  
jkrichma@uci.edu

## Abstract

This paper introduces the modulated Hebbian plus Q network architecture (MOHQA) for solving challenging partially observable Markov decision processes (POMDPs) deep reinforcement learning problems with sparse rewards and confounding observations. The proposed architecture combines a deep Q-network (DQN), and a modulated Hebbian network with neural eligibility traces (MOHN). Bio-inspired neural traces are used to bridge temporal delays between actions and rewards. The purpose is to discover distal cause-effect relationships where confounding observations and sparse rewards cause standard RL algorithms to fail. Each of the two modules of the network (DQN and MOHN) is responsible for different aspects of learning. DQN learns low level features and control, while MOHN contributes to the high-level decisions by bridging rewards with past actions. The strength of the approach is to support a DQN standard framework when temporal difference errors are difficult to compute due to non-observable states. The system is tested on a set of generalized decision making problems encoded as decision tree graphs that deliver delayed rewards after key decision points and confounding observations. The simulations show that the proposed approach helps solve problems that are currently challenging for state-of-the-art deep reinforcement learning algorithms.

## Introduction

Challenging problems for reinforcement learning are those in which observations do not reveal the Markov states of the environment. Such problems are also known as partially observable Markov decision problems (POMDP) (Sondik 1971). One solution is to use the history of observation as state, transforming to problem to MDP and thus enabling RL to learn a state-action value function (Mnih et al. 2015; Sutton and Barto 2018). LSTMs were successfully used in deep recurrent Q-learning to solve some types of POMDP such as flickering Atari (Hausknecht and Stone 2015; Heess et al. 2015; Mirowski et al. 2016).

The history of observations, however, is not always sufficient to efficiently solve a POMDP. In fact, if the observa-

tions derive from a large set, a sequence of observations is unlikely to repeat, and therefore the derived MDP is very large; moreover, if the time gap between actions and reward has a variable delay, intervening observations also result in a large space of histories. These conditions can be intuitively understood as problems in which input data across a time window is not equally important to inform the decision process and maximize reward. Thus, rather than the observation history, other approaches to solve POMDPs rely on a belief system. E.g., (McAllister and Rasmussen 2017) propose an approach based on the well known model-based PILCO algorithm for continuous control. A variational autoencoder is used to update a belief system in (Igl et al. 2018) and reported improved performance over (Hausknecht and Stone 2015) in POMDPs such as the flickering ATARI. (Azizzadenesheli, Lazaric, and Anandkumar 2017) introduced spectral methods in reinforcement learning to solve POMDPs problems. (Doshi-Velez et al. 2015) used Bayesian nonparametric representations for distinguishing between separate states to help with appropriate action selection.

In this paper, we propose a new way to cope with confounding stimuli and delayed rewards by augmenting a DQN architecture with a single layer reward-modulated Hebbian network with neural eligibility traces. This new deep RL architecture can discriminate between pivotal decision points and irrelevant or confounding observations, thus gaining a learning advantage in RL problems with delayed rewards and confounding observations. A modulated Hebbian network with neural eligibility traces (MOHN) is employed to reconstruct observation-actions-rewards sequences with variable delays in the cause-effect chain of events. The ability of MOHN to bridge temporal gaps between causing events and rewards was demonstrated in a spiking neural model in (Izhikevich 2007), and an equivalent model for rate-based neurons was shown effective in simulation (Soltoggio and Steil 2013) and robotics applications (Soltoggio et al. 2013a; Soltoggio et al. 2013b).

Traces is not a new concept and it has been explored in the past reinforcement learning literature (Sutton and Barto 2018; Munos et al. 2016). The main difference between traces in re-

inforcement learning and neural traces in MOHN (Izhikevich 2007; Soltoggio and Steil 2013) is in the different computational framework that creates and used them: in TD( $\lambda$ ), traces are incremented by the value of the gradient  $\nabla v(S_t, \mathbf{w}_t)$  that, with linear approximation, corresponds to the feature vector  $\mathbf{x}_t$ . In MOHN, increments are instead derived from a cause-effect neural dynamics inspired by the STDP learning rule (Markram et al. 1997). An augmented version of STDP with neuromodulation (Izhikevich 2007) can be used in a Hebbian network with rate-based neurons (Soltoggio et al. 2013a) to derive cause-effect relationships. Finally, TD error is not easily computed in POMDP because states might not be defined or correctly identified, therefore MOHN use the raw reward signal, and not the difference between actual and expected reward. Recurrent modulated networks (Izhikevich 2007; Soltoggio et al. 2013a), can learn to compute the difference between actual and expected reward, but they are nevertheless fed with raw reward signals.

Exploiting the properties of reward-modulated Hebbian networks, we propose a modulated Hebbian plus Q network architecture (MOHQA) for deep reinforcement learning problems. The architecture is composed of two parts: a standard DQN network, and a modulated Hebbian network (MOHN), parallel to the Q-network head that contributes to decision making. The key idea is that the modulated Hebbian network can learn distal associations, which allow the network to ignore time gaps and confounding observations that occur between actions and rewards. In other words, the MOHN infers associations between inputs, outputs, and rewards, across multiple time steps, thus bypassing the need to compute a TD error, which maybe uncertain due partially observable states. The DQN shares the feature extraction convolutional layers with the Hebbian network. Thus, while DQN (Mnih et al. 2015) can learn useful features even in problems that it cannot solve because of partial observability, the MOHN contributes to the decisions of the DQN when TD error is misleading due to confounding observations.

Two unique aspects of the traces used in the MOHQA are: (i) traces are used only in the network head and (ii) traces are sparse (or rare). The first point (i) implies that traces are used to associate high level features with decisions: this principle implicitly assumes that distal cause-effect relationships exist at high level features, rather than at the input pixel level. Point (ii) implies that the eligibility of weights is increased only in a small percentage of the total number, ensuring that credit is assigned to a small subset of weights. This is critical to maintain stability with raw reward signals when TD errors cannot be computed.

The architecture is tested in a set of generalized reward-based decision problems that include POMDPs with delayed rewards and confounding observations. Tests include comparisons with a baseline DQN, QRDQN+LSTM (Hausknecht and Stone 2015) and A2C (Mnih et al. 2016). Initial tests shows that the MOHQA solves POMDPs where the baseline algorithms fail. The proposed approach is the first application of a combined Hebbian and DQN network to implicitly learn a belief system and address challenging TD computation in the presence of partially observable Markov states.

## A set of POMDP problems with distal rewards and confounding observations

Assume an environment where key decision points, in which actions are critical, occur occasionally and are separated by wait states during a simple and fixed policy is required, e.g., action wait. This is a fairly common case in robotics applications and games. This scenario is implemented in this work with a configurable tree graph (CT-graph) that encodes a partially observable MDP and returns observations of two main types: *decision points* (where the graph branches in multiple sub-graphs) and *wait states* (where the tree-graph does not branch). Actions are also of two types: *wait-actions* and *act-actions*. The CT-graph is designed to be a challenging problem for current state-of-the-art RL approaches. The CT-graph results in (1) the sparsity of the reward, (2) the non-observability of the MDP and (3) a large number of confounding observation.

A reward is located at one particular leaf node in the tree graph. The agent is required to perform wait-actions while in a wait state and choose from a set of act-actions while at a decision point. The choice of a specific act-action determines the path that the agent follows along the tree. While at a wait state, the agent receives observations that can be seen as confounding observations because only the wait-action is ever required in a wait state (only one wait-action is used in the current setup). Wait states lead to themselves with a delay probability  $p$  or to the next state in the sequence with probability  $1 - p$ . At each decision point there are  $b$  options corresponding the branches in the sub-graphs. of a tree graph. The number of consecutive decision points is the depth  $d$  of the tree graph. The environment has an optimal sequence of actions that leads to one unique leaf of the tree graph that returns a reward of one. The branch factor  $b$ , the depth  $d$ , the delay probability  $p$ , and the sets of observations are configurable parameters, making this problem a blueprint for a large set of benchmarks, from simple to extremely difficult problems for medium to large sizes graphs (Fig. 1).

For each type of states, the environment provides either deterministic or stochastic observations, but all from the specific subsets of  $\mathcal{O}$  associated with one state type: thus, different states of the same type can provide the same observations. Referring to Fig. 1(B), S1, S3 and S4 (wait states) may all provide the same observation or different observations from the same set, which makes the problem a POMDP<sup>1</sup>. While a standard input size for DRL is the  $84 \times 84$  image size used with the ATARI platform, we implemented a smaller  $12 \times 12$ -sized set that allows for a considerably faster simulation while nevertheless requiring a feature extraction phase. The images are single-channel scaled up and rotated  $4 \times 4$  checker patterns of low-medium-high values (Fig. 1(C)). Such choice of images was made to require feature learning and test deep RL algorithm while maintaining low computational requirements.

While the problem is simple in the mathematical formulation, it can be made very difficult for RL to solve due to large reward sparsity and confounding observations. In fact, in the

<sup>1</sup>Source code for the CT-graph provided at <https://github.com/--anonymised>

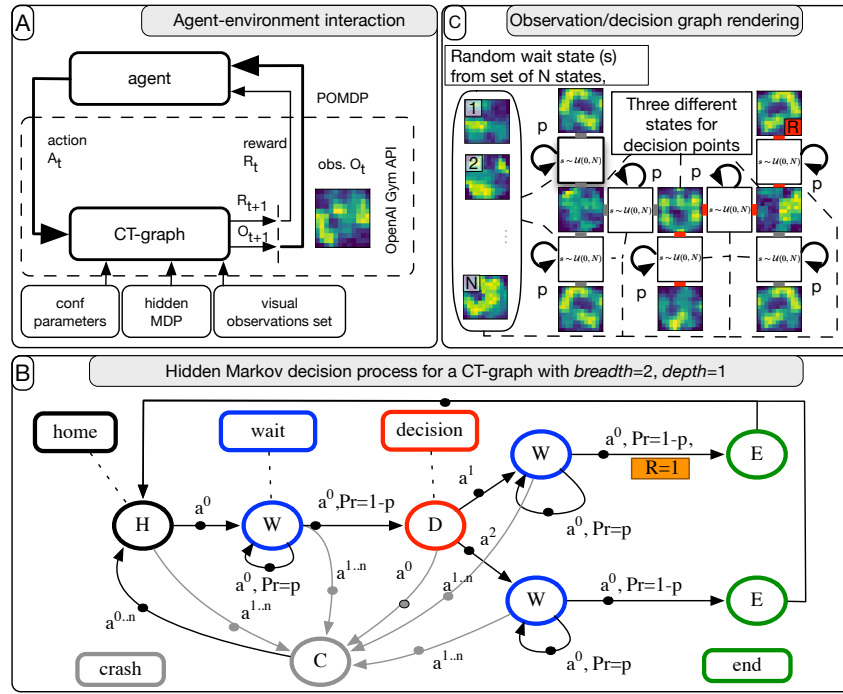


Figure 1: The CT-graph problem. (A) The agent-environment interaction is similar to the standard RL with the difference that the environment provides observations. (B) Representation of the hidden Markov process: the wait-action  $a^0$  is required at wait states, while act-actions  $a^1$  to  $a^2$  are required at decision points. The panel shows a graph with one single decision point. (C) Graphical representation of the observations and decision in a maze-like rendering: wait states and decision points can be seen as wait states and decision points in a CT-graph.

most complex graph that we tested random exploration results in a reward only once in 84,000 episodes, or 2.7M steps (depth 2, branch 2, probability ( $p$ ) 0.1). Such a condition was sufficient to make most advanced RL algorithms currently known ineffective.

**Non-observability and wait.** Wait states and decision points alternate while following a branch of the tree graph, and similarly the observations that depend on such states alternate and reoccur along the graph. As a result, neither the observations, nor the state types provide an observable MDP. The delay probability  $p$  of transitioning from a wait state to a decision point determines the expected delay between decision points, and between the last decision point and the reward at the end of the episode. Such a setup represents a decision-making process in which confounding observations (waiting state) are more common, than decision points. This situation can occur for example when a robot is traversing a new building. Corridors of a building may result in similar, seemingly random observations due to simple similarities or noise in the various sensors, while the critical decision are taken at specific landmarks. A list of all states used in CT-graph for this experiment is available in supplementary materials.

**Comparison to other RL benchmarks.** Compared to other RL benchmarks such as various games (Atari,

Minecraft) or control benchmarks (muJoCo, lunar lander), the CT-graph differs in two aspects i) decision making is significantly more complex in a CT-graph and ii) the CT-graph is visually simpler. For example, the majority of actions in the CT-graph result in the episode termination with a reward of 0, while in other benchmarks the agent can take several actions before a termination occurs. Moreover, in some Atari games (e.g., breakout) the agent is likely to stumble across a reward with a relatively high probability and a short sequence of actions. On the contrary, in the CT-graph, the agent has to complete a longer sequence of actions to reach a reward, which is consequently more sparse. The high sparsity of the reward makes exploration less effective. Secondly, while our visual input is simpler than other benchmarks, some important aspects of complexity of the visual input are retained such as states associated with decisions are similar to states associated with waiting points, thus very similarly looking states require different decisions.

## The modulated Hebbian plus Q network architecture (MOHQA)

The proposed architecture (MOHQA) is composed of two main parts: a deep Q-network (Mnih et al. 2015) (DQN), and a modulated Hebbian network (MOH) that is plugged into the Q-network as a parallel unit to the DQN head (Fig. 2).

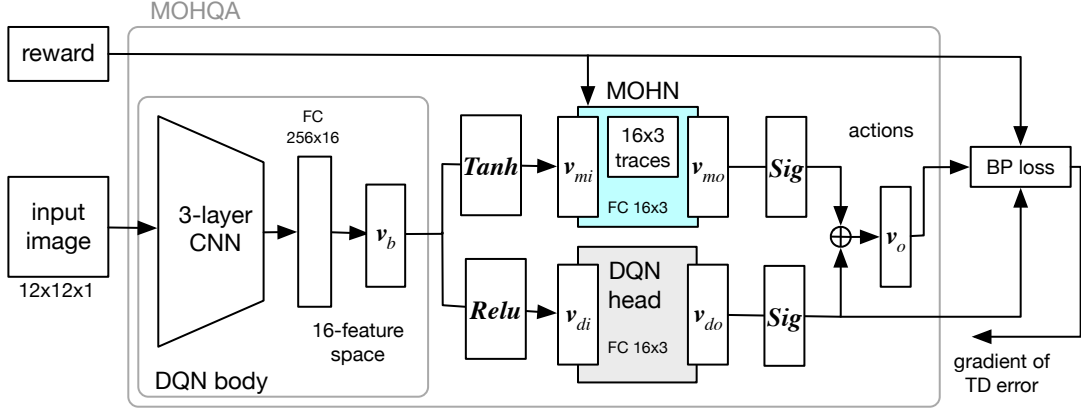


Figure 2: Graphical representation of the MOHQA. The DQN body feeds the feature space to both the DQN head and the MOHN. The action-value vector is the sum of the outputs of the two heads. The learning in the MOHN is regulated by modulated Hebbian plasticity. The learning in the DQN network is performed by back propagation.

Layer	In channel size	Out channel size	Kernel size	Stride
1st convolution layer	1	4	5	1
2nd convolution layer	4	8	3	1
3rd convolution layer	8	16	3	1
1st linear layer	256	16	N/A	N/A
2nd linear layer	16	3	N/A	N/A

Table 1: Sizes of the convolutional layers of the DQN body for the 12x12 image data of the CT-graph.

### DQN description

The DQN follows the standard implementation (Mnih et al. 2015). A standard DQN is used to approximate the optimal Q-value function, or optimal value-action function, defined as

$$Q(s, a) = \max_{\pi} \mathbb{E}[r_t + \gamma r_{t+1} + \gamma^2 + \dots | s_t = s, a_t = a, \pi] \quad (1)$$

where  $r_t$  is a reward at time  $t$ ,  $s_t$  is a state at time  $t$ ,  $a_t$  is an action at time  $t$  and  $\pi$  is the policy. To solve instability issues caused by representing action-value pairs with the network, (Mnih et al. 2015) proposed two innovations i) experience replay and ii) a target network that is only periodically updated. The parameters of the target and base network are  $\Phi^-$  and  $\Phi$ . The parameters  $\Phi^-$  are updated with  $\Phi$  every  $K$  steps.

The output of the DQN body is a set of features that are used as input to both the MOHN and DQN heads. The layers and sizes of the DQN body are summarized in Table 1. The DQN head is the final layer of the DQN network. It interprets the features to produce Q-values. Both DQN head and DQN body are trained by back propagation to minimize the TD

error (Mnih et al. 2015).

### Associating stimulus-action pairs with distal rewards by means of MOHN

The MOHN in this work is an adaptation of a bio-inspired, unsupervised and modulated Hebbian network proposed in (Izhikevich 2007; Soltoggio and Steil 2013). In those studies, those networks were shown to cope with sparse rewards outside a RL framework, i.e. when neither states nor TD errors are defined. These assumptions are useful when an agent cannot infer the state of the MDP, and thus a TD error cannot be correctly computed and used to propagate the Q function updates. This is generally true even with memory-augmented DQN such as RDQN: in fact, if the history of observations maps to a large space due to stochastic observations, learning history-action values is ineffective. The confusion is a result of memorized observations appearing at different positions throughout the graph at different episodes, thus memorized memorized cannot be used to determine which action to take in the next state. For example in one episode observation appearing just before decision point (implying agent should take act-action), can appear in front of another wait state in the next episode, confusing the decision making. The MOHN solves this problem by using a learning rule based on modulated Hebbian with eligibility traces that uses raw reward signals. The result is that observations-action pairs are associated with later rewards by means of traces that update the weights that caused an action and “ignore” intervening events between actions and rewards.

### STDP-inspired plasticity and neural eligibility traces (MOHN)

The neural traces used in this study implement two principles: (i) causal relationships between observation and actions, and (ii) sparse correlations. The causal relationship are derived by applying the Hebbian multiplication rule to successive, rather than simultaneous, simulation steps, so that Hebbian terms captures the contribution of a presynaptic activity to

the activity of a postsynaptic neuron, similarly to the STDP rule. This is also sometimes called an asymmetrical learning window (Kempster, Gerstner, and Van Hemmen 1999). Sparse correlations are explicitly imposed by selecting the top  $\theta\%$  and bottom  $\theta\%$  of correlations/decorrelations (Soltoggio et al. 2013a). A modified Hebbian term  $\Theta$  between a presynaptic neuron  $pre$  and a postsynaptic neuron  $post$  is updated according the equation:

$$\Theta_{pre \rightarrow post}(t) = \begin{cases} 1 & \text{if } v_{pre}(t-1) \cdot v_{post}(t) \text{ is in top } \theta\% \\ -1 & \text{if } v_{pre}(t-1) \cdot v_{post}(t) \text{ is in bottom } \theta\% \\ 0 & \text{otherwise} \end{cases} \quad (2)$$

where  $v_{pre}$  and  $v_{post}$  are the output values of the pre and postsynaptic neurons, equivalent to the input and output layers in the MOHN. The input to the MOHN,  $\mathbf{v}_{mi}$  is the output of the DQN body  $\mathbf{v}_b$  (Fig. 2) minus its own running average to enhance the detection of changes in the feature space. The traces in the  $\Theta$  and decay  $E$  decay with time with a time constant  $\tau_E$

$$\dot{E}(t) = -E(t)/\tau_E + \Theta(t) \quad (3)$$

The modulatory signal is the reward plus a small baseline modulation, i.e.,  $r(t) + b$ , and is used to multiply the traces to obtain the weight update:

$$\Delta \mathbf{w}(t) = (r(t) + b) \cdot E(t) \quad (4)$$

The weights are clipped in the interval  $[-1, 1]$  to contain Hebbian updates (Miller and MacKay 1994; Soltoggio and Stanley 2012).

It is worth noting that the MOHN is capable of intrinsic exploration and exploitation dynamics. Exploitation derives from the typical Hebbian dynamics that reinforces established behaviors (Hebb 2005) by leading weights to saturation (Miller and MacKay 1994). Behaviors that do not lead to reward, instead, cause weight depression that consequently leads to noise-driven exploration. Noise in the system can be added both at the input level (noise on the pixels of the image) or at feature levels. In both cases, noises has the role to facilitate exploration of weight configurations (Soltoggio and Stanley 2012).

Finally, the output of the MOHN,  $\mathbf{v}_{mo}$ , is computed as:

$$\mathbf{v}_{mo} = \Gamma(\tanh(\sum_j (\mathbf{w} \cdot \mathbf{v}_{mi}))) \quad (5)$$

where  $\Gamma$  is a function that returns a one-hot vector with the 1 value at the index of the maximum value, and  $\sigma$  is a sigmoid function. The one-hot function has the purpose to facilitate the increase of the traces for the weights that are afferent to the action-triggering neuron.

## Integration

The idea to sum the output of DQN head with the output of the MOHN is to provide the overall architecture a set of additional high level hints that highlight cause-effect relationships across time gaps to help decisions when standard DQN fails. Thus, the MOHQA Q-values,  $\mathbf{v}_o$ , are defined as

$$\mathbf{v}_o = \mathbf{v}_{do} + \mathbf{v}_{mo} = \mathbf{v}_{do} + Q(s, A; \Phi_i^-) \quad (6)$$

where  $s$  indicates that an observation is used to approximate the state, even when this is incorrect due to partial observability. As in standard approaches, the action is chosen as

$$a_b = \arg \max_a (\mathbf{v}_o) \quad (7)$$

Crucially, the loss function is computed using the difference between best action as indicated by the q-value of sum of DQN and MOHQA and q-value indicated by the DQN:

$$L(\Phi) = \mathbb{E} \left( r + \gamma \mathbf{v}_o(s', a_b, \Phi_i^-) - Q(s, a; \Phi_i) \right)^2 \quad (8)$$

## Results

This section reports the analysis of how the MOHQA uses the features to solve the POMDP problems and then presents a comparison of the performance with the DQN, QRDQN+LSTM, REINFORCE and A2C algorithms.

**Analysis of feature learning.** To better understand the need for a new loss function  $L(\Phi)$ , three experiments are performed (Fig. 3) to show feature learning by DQN (A) in a one-decision-point CT-graph, (B) in a two-decision-point CT-graph with traditional loss function, (C) and finally a two-decision-point CT-graph with the newly proposed loss function. In the first experiment, the baseline DQN attempted to learn a CT-graph with one decision point and two wait states, one before and one after the decision point. Fig. 3(A) shows the learned feature space output throughout one episode. As expected, DQN learns similar high level features from different observations if those require the same action. In particular, wait states that require the wait-action  $a^0$  are distinguishable from decision points that require act-actions. However, TD learning can not propagate the reward values backwards because the wait states (before and after the decision point) are not distinguished.

A similar situation is observed in a longer CT-graph with two decision points in Fig. 3(B). In this case, the two decision points had unique observations, thus making the problem observable, but only at decision points. DQN learns the same features for wait states and decision points. This is reasonable because these two state types require either action  $a^0$  (wait state) or actions  $a^1$  or  $a^2$  in the decision point. However, not only the observations prevents propagation of the TD error, but the feature space does not allow to distinguish between the first and second decision point. This confusion between first and second decision point highlights an interesting consideration: if DQN cannot learn the path to the reward, it cannot also learn the separate features that would enable correct decisions.

Finally, in the third experiment, the MOHQA is used on the same two decision-point CT-graph. In Fig. 3(C) the feature space clearly shows a difference between the first and second decision point. The MOHQA, by suggesting optimal actions to the DQN, was able to also lead the DQN to learn different features for different decision points, which DQN alone could not achieve. In this last test, the output values reveal the inner working of the MOHQA architecture: DQN suggests the wait-action at wait states, and expresses equal preferences

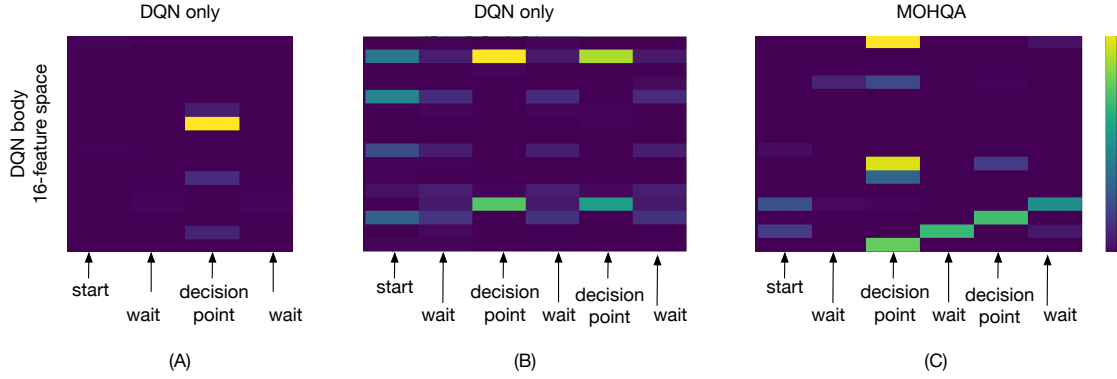


Figure 3: Features learned by the DQN body without and with the MOHQA. (A) In a one-decision-point CT-graph, DQN correctly learns that the observations before and after the decision points are the same, but so the TD error cannot be computed. (B) In a two decision-points CT-graph, DQN learns features that are the same for wait states and decision points: this allows navigation to a leaf node but random actions are taken at decision points. (C) The MOHQA helps selecting the correct actions, and a consequence, DQN learns different features for the two different decision points.

for both act actions  $a^1$  and  $a^2$ . The MOHN contributes by biasing the decision towards the act-action (either  $a^1$  or  $a^2$ ) that is associated with the future reward.

### Comparisons

Simulations were performed for a range of CT-graphs and compared with benchmark algorithms<sup>2</sup>. For all simulations, we used a baseline modulation  $b = -0.0001$ , a sparse correlation threshold  $\theta = 13\%$  and a decay factor  $\tau_E$  of 14 and 48 steps for the one-decision-point and two-decision-point CT-graph.

**One-decision-point CT-graph.** In a one-decision-point CT-graph (Fig. 4)(b) with variable delay ( $p = 0.5$ ), all RL algorithms solve a MPD version (all observations are unique) (Fig. 4(a)). In Fig. 4(b), the CT-graph is made POMDP by removing uniqueness from the wait states. This is the case where confounding observations affect the problem. The MOHQA is able to solve the problem while the other approaches do not. Note that the simplest of the CT-graphs (Fig. 4 (a) and (b) and Fig. 5(a)) do not require a feature extractor due to limited number of states used in the problem. The feature extractor is kept for a generality of the approach and for fair comparison with more complex CT-graphs.

**Two-decision-points CT-graph.** For the two-decision-points CT-graph, three tests are performed, i) fully MDP with  $p = 0$  (Fig. 5(a), ii) POMDP, where a wait state produces one of 64 observations, and  $p$  is 0.5 (Fig. 5(b) and iii) POMDP, where a wait state produces one of the 64 observations, and  $p$  is 0.9 (Fig. 5(c)). The two-decision-points CT-graph (Fig. 5) shows very similar trends to one-decision-point CT-graph, but reveals the increased complexity of the problem with the baseline algorithms failing.

<sup>2</sup>The simulation code will be made available at <https://github.com/pladosz/MOHQA.git>.

### Discussion

The deep reinforcement learning problems posed in this paper appear trivial, and yet, state-of-the-art RL algorithms struggle to find good solutions. The particular and yet common challenge derives from a non-Markov problem in which the history might not be useful to reconstruct the hidden MDP due to the large space of possible histories. It is worth noting that, although POMDP, the CT-graph was configured to allow for solutions with agents that do not have memory. This is an interesting consideration because it is assumed that DQN cannot solve a hidden MDP without a memory unit (e.g. LSTM), but the QRDQN+LSTM baseline shows that such an approach also struggles. The memory based approach is likely not to learn correctly due the challenge of propagating TD-error, essential to train the LSTM, and therefore it fails to learn distinguishing features for different observations.

The current proof-of-concept MOHQA is tested on a limited set of POMDP problems and compared with a limited number of benchmark algorithms. Further tests with other POMDP problems, e.g. the Morrison water maze and some ATARI games, will be essential to test the full potential of the MOHQA. Yet, the present work suggests that a fundamentally simple test of POMDP deep RL problems casts insights on the challenging problem of learning simultaneously a feature space and an policy with delayed rewards and confounding observation.

The proposed architecture, while proving effective and posing a new learning paradigm, has some limitations. The MOHQA is more complex than a standard DQN network. However, to the best of the authors' knowledge, this is the first successful attempt to combine a modulated unsupervised Hebbian network with a DQN network. The MOHQA solves a POMDP without memory because non-observability is limited to the wait states, while the observations from decision points corresponds to states. In future developments, a promising direction is to add memory to the MOHQA to enable it to solve even more complex POMDP problems. The time constant of the traces determines how far back re-



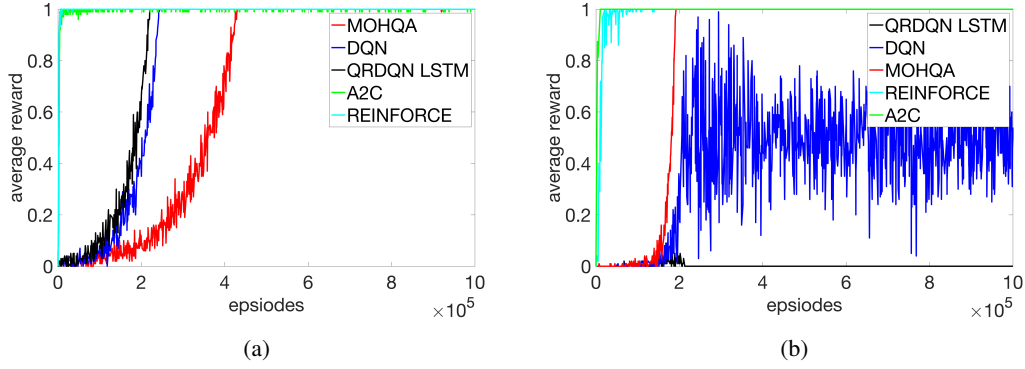


Figure 4: Performance on the one-decision-point CT-graph. (a) In an MDP benchmark test (each observation is unique, and therefore reveals a unique state,  $p = 0$ ): as expected, all algorithms learn the optimal behavior. (b) POMDP ( $p = 0.5, N = 64$ ): wait states provide similar observations: DQN learns to explore the graph and takes random decision, therefore collects 50% of the reward. The variable delay maybe the cause of the poor performance of the QRDQN+LSTM.

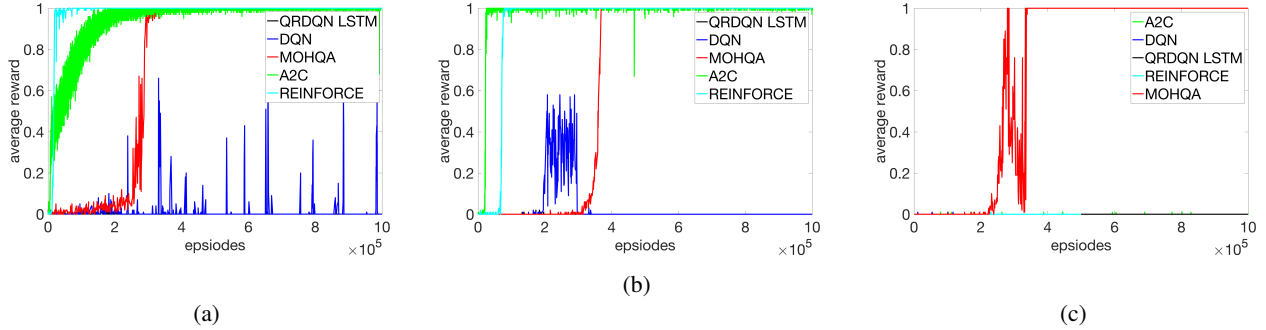


Figure 5: Performance on the two-decision-points CT-graph. (a) With a fixed delay duration ( $p = 0$ ) and confounding observations, only A2C and the proposed approach appears to learn a good strategy, while other approaches struggle. (b) The same problem with a variable delay duration ( $p = 0.5$ ) poses even more severe challenges to the baseline algorithms. (c) Graph with delay probability of  $p = 0.9$ , is an extremely sparse reward POMDP problem and is only solved by proposed algorithm.

wards can be associated with observation-actions pairs. A fast decaying trace cannot capture too long delays; a slow decaying trace means that too many observations-action pairs are credited, resulting in either slow or unstable learning.

Finally, an interesting consideration is that the MOHN appears to be instrumental to guide DQN to learn useful features. Due to the confounding observations that are provided during wait states, the baseline algorithms struggle to learn useful features of the decision points, which are instrumental to inform an optimal policy. Thus, learning the appropriate features depend on the actions which in turn depends on the feature. While this chicken and egg problem is typical in deep reinforcement learning, the proposed MOHQA appears to facilitate the process of guiding the learning of useful features by discovering cause-effect relationships and offering guidance to the DQN underlying architecture.

## Conclusion

This paper proposed a new neural architecture (MOHQA) for deep reinforcement learning. The key novelty is the in-

tegration, of a standard DQN architecture, and a modulated Hebbian learning network with neural eligibility traces. The objective was to provide an RL agent with the ability to ignore confounding observation during delays and associate key cause-effect relationships to delayed rewards. The parallel architecture was shown to enhance the standard DQN with the ability to learn in challenging POMDPs where a number of state-of-the-art approaches fail (DQN, A2C, QRDQN+LSTM). While this is the first proof-of-concept study to propose a combined Hebbian and a backpropagation-learned architecture for deep reinforcement learning, the promising results encourage further tests on a wider range of standard deep RL benchmarks.

**Acknowledgments** This material is based upon work supported by the United States Air Force Research Laboratory (AFRL) and Defense Advanced Research Projects Agency (DARPA) under Contract No. FA8750-18-C-0103.

Any opinions, findings and conclusions or recommendations expressed in this material are those of the author(s) and do not necessarily reflect the views of the United States Air

## References

- [Azizzadenesheli, Lazaric, and Anandkumar 2017] Azizzadenesheli, K.; Lazaric, A.; and Anandkumar, A. 2017. Experimental results : Reinforcement Learning of POMDPs using Spectral Methods. *JMLR: Workshop and Conference Proceedings* 49:1–64.
- [Doshi-Velez et al. 2015] Doshi-Velez, F.; Pfau, D.; Wood, F.; and Roy, N. 2015. Bayesian nonparametric methods for partially-observable reinforcement learning. *IEEE Transactions on Pattern Analysis and Machine Intelligence* 37(2):394–407.
- [Hausknecht and Stone 2015] Hausknecht, M., and Stone, P. 2015. Deep recurrent Q-learning for partially observable MDPs. In *2015 AAAI Fall Symposium Series*.
- [Hebb 2005] Hebb, D. O. 2005. *The organization of behavior: A neuropsychological theory*. Psychology Press.
- [Heess et al. 2015] Heess, N.; Hunt, J. J.; Lillicrap, T. P.; and Silver, D. 2015. Memory-based control with recurrent neural networks. *arXiv preprint arXiv:1512.04455*.
- [Igl et al. 2018] Igl, M.; Zintgraf, L.; Le, T. A.; Wood, F.; and Whiteson, S. 2018. Deep variational reinforcement learning for POMDPs. In Dy, J., and Krause, A., eds., *Proceedings of the 35th International Conference on Machine Learning*, volume 80 of *Proceedings of Machine Learning Research*, 2117–2126. Stockholmsmässan, Stockholm Sweden: PMLR.
- [Izhikevich 2007] Izhikevich, E. M. 2007. Solving the distal reward problem through linkage of stdp and dopamine signaling. *Cerebral cortex* 17(10):2443–2452.
- [Kempster, Gerstner, and Van Hemmen 1999] Kempster, R.; Gerstner, W.; and Van Hemmen, J. L. 1999. Hebbian learning and spiking neurons. *Physical Review E* 59(4):4498.
- [Markram et al. 1997] Markram, H.; Lübke, J.; Frotscher, M.; and Sakmann, B. 1997. Regulation of synaptic efficacy by coincidence of postsynaptic apss and epsps. *Science* 275(5297):213–215.
- [McAllister and Rasmussen 2017] McAllister, R., and Rasmussen, C. E. 2017. Data-efficient reinforcement learning in continuous state-action Gaussian-POMDPs. In Guyon, I.; Luxburg, U. V.; Bengio, S.; Wallach, H.; Fergus, R.; Vishwanathan, S.; and Garnett, R., eds., *Advances in Neural Information Processing Systems 30*. Curran Associates, Inc. 2040–2049.
- [Miller and MacKay 1994] Miller, K. D., and MacKay, D. J. 1994. The role of constraints in hebbian learning. *Neural Computation* 6(1):100–126.
- [Mirowski et al. 2016] Mirowski, P.; Pascanu, R.; Viola, F.; Soyer, H.; Ballard, A. J.; Banino, A.; Denil, M.; Goroshin, R.; Sifre, L.; Kavukcuoglu, K.; et al. 2016. Learning to navigate in complex environments. *arXiv preprint arXiv:1611.03673*.
- [Mnih et al. 2015] Mnih, V.; Kavukcuoglu, K.; Silver, D.; Rusu, A. A.; Veness, J.; Bellemare, M. G.; Graves, A.; Riedmiller, M.; Fidjeland, A. K.; Ostrovski, G.; et al. 2015. Human-level control through deep reinforcement learning. *Nature* 518(7540):529.
- [Mnih et al. 2016] Mnih, V.; Badia, A. P.; Mirza, M.; Graves, A.; Lillicrap, T.; Harley, T.; Silver, D.; and Kavukcuoglu, K. 2016. Asynchronous methods for deep reinforcement learning. In *International conference on machine learning*, 1928–1937.
- [Munos et al. 2016] Munos, R.; Stepleton, T.; Harutyunyan, A.; and Bellemare, M. G. 2016. Safe and efficient off-policy reinforcement learning. In *Proceedings of the 30th International Conference on Neural Information Processing Systems*, NIPS’16, 1054–1062. USA: Curran Associates Inc.
- [Soltoggio and Stanley 2012] Soltoggio, A., and Stanley, K. O. 2012. From modulated hebbian plasticity to simple behavior learning through noise and weight saturation. *Neural Networks* 34:28–41.
- [Soltoggio and Steil 2013] Soltoggio, A., and Steil, J. J. 2013. Solving the distal reward problem with rare correlations. *Neural computation* 25(4):940–978.
- [Soltoggio et al. 2013a] Soltoggio, A.; Lemme, A.; Reinhart, F.; and Steil, J. J. 2013a. Rare neural correlations implement robotic conditioning with delayed rewards and disturbances. *Frontiers in neurorobotics* 7:6.
- [Soltoggio et al. 2013b] Soltoggio, A.; Reinhart, F.; Lemme, A.; and Steil, J. 2013b. Learning the rules of a game: neural conditioning in human-robot interaction with delayed rewards. In *2013 IEEE Third Joint International Conference on Development and Learning and Epigenetic Robotics (ICDL)*, 1–6. IEEE.
- [Sondik 1971] Sondik, E. J. 1971. The optimal control of partially observable markov processes. Technical report, STANFORD UNIV CALIF STANFORD ELECTRONICS LABS.
- [Sutton and Barto 2018] Sutton, R. S., and Barto, A. G. 2018. *Reinforcement learning: An introduction*. MIT press.